

(Supporting Information)

**In-situ synthesis of Ni nanofibers via vacuum thermal reduction and their
efficient catalytic properties for hydrogen generation**

Qinglong Fu^{1,2,#}, Pan Yang^{1,#}, Jingchuan Wang¹, Hefang Wang^{2,*}, Lijun Yang^{1,*}, Xiaochong Zhao^{1,*}

¹ Institute of Materials, China Academy of Engineering Physics, Jianguo 621908, China

² School of Chemical Engineering and Technology, Hebei University of Technology, Tianjin
300130, China

*Corresponding author email: zhaoxiaochong@caep.cn (X. Zhao), sherry_yang0710@163.com (L.
Yang), whf0618@163.com (H. Wang)

Results and discussion

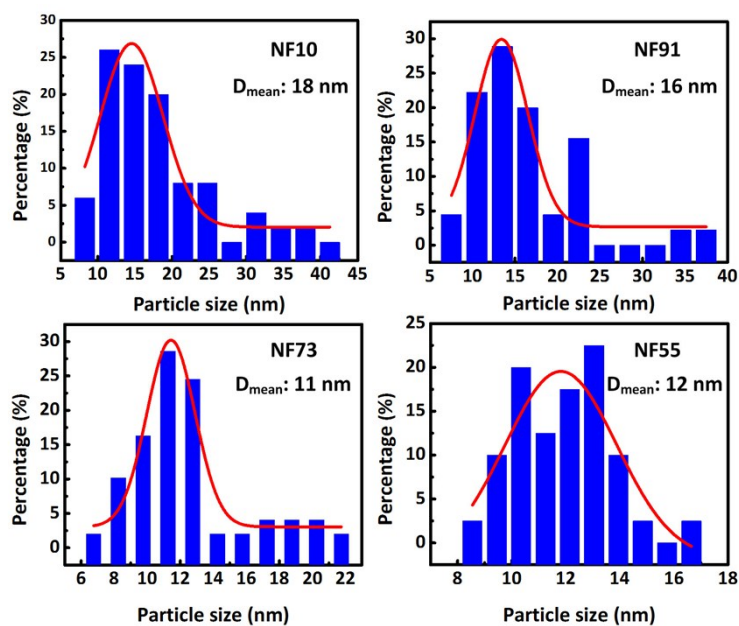


Fig. S1 Histograms of Ni particle size distributions of NF10, NF91, NF73 and NF55 nanofibers.

Histograms of the Ni particle size distributions were obtained by taking measurements 50 Ni particles from each TEM image using image analysis software (Nano Measurer 1.2). The statistical results are shown in Fig. S1.

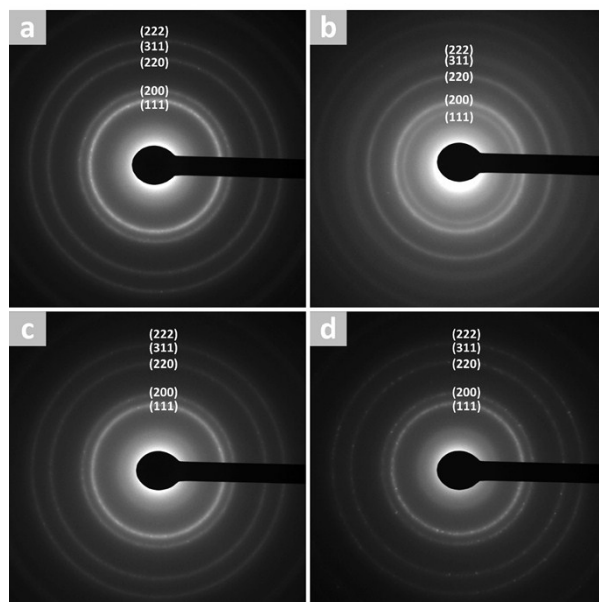


Fig. S2 SAED patterns of (a) NF10, (b) NF91, (c) NF73 and (d) NF55.

As shown in Fig. S2, the selected area electron diffraction (SAED) patterns of four Ni nanofibers consist of recognizable diffraction rings, suggesting that Ni nanofibers have a

polycrystalline nature. The squares of radius of the (111), (200), (220), (311), and (222) diffraction rings are in good agreement with 3: 4: 8: 11: 12, which indicate that Ni nanocrystals have face center cubic structure.

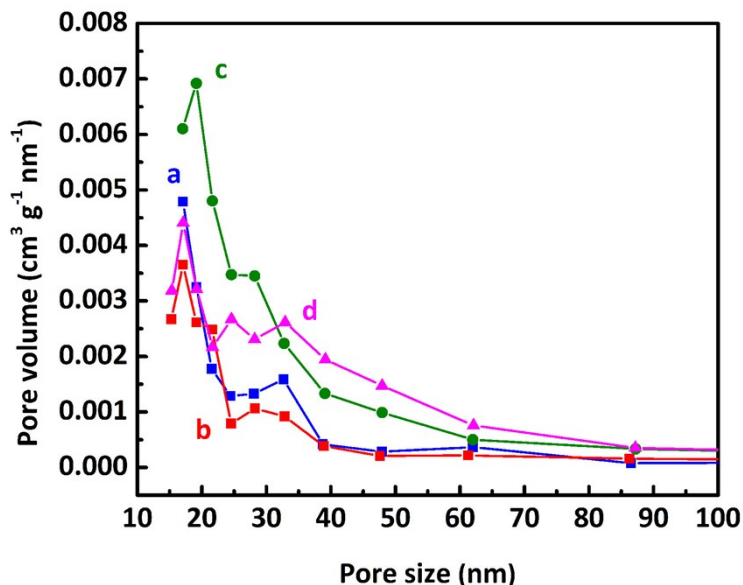


Fig. S3 BJH pore size distributions of (a) NF10, (b) NF91, (c) NF73 and (d) NF55.

The pore size distribution curves indicate that there are two types of pores. The small pores (about 17-19 nm) are considered as mesopores of Ni nanofibers materials. While the large pores with a broad distribution (about 24-38 nm) may be deemed to the aggregated pores between the Ni nanofibers.

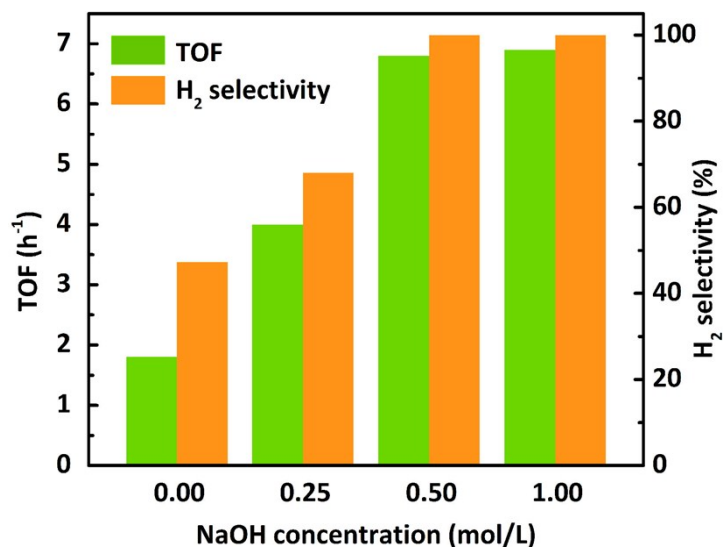


Fig. S4 Effect of NaOH concentration on TOF and selectivity to H₂ in the reaction of hydrous hydrazine decomposition catalyzed by NF73 at 333K with different NaOH concentration (NF73 /N₂H₄·H₂O = 0.5).

As shown in Fig. S4, the H₂ selectivity and catalytic activity of NF73 catalyst for the hydrous hydrazine decomposition increased with the concentration of NaOH solution until the high concentration NaOH solution (0.5 M) was used. After that, further increasing the concentration of NaOH, there was no obvious effect on the H₂ selectivity and catalytic activity. The existence of NaOH decreases the concentration of N₂H₅⁺ (N₂H₅⁺ + OH⁻ → N₂H₄ + H₂O), which is also promotes the generation of H₂.¹ In addition, rate-determining deprotonation step (N₂H₄ → N₂H₃^{*} + H^{*}) of hydrous hydrazine decomposition could be accelerated in the presence of OH⁻.²

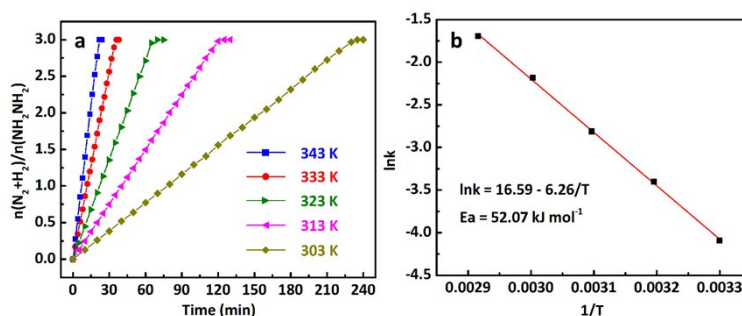


Fig. S5 (a) Time-course plots for the decomposition of N₂H₄·H₂O over NF73 at different temperatures. (b) Arrhenius plots of $\ln k$ versus $1/T$ during the N₂H₄·H₂O decomposition over NF73 at different temperatures.

(NF73 /N₂H₄·H₂O = 0.5, 0.5 M NaOH).

Fig. S5 shows a series of catalytic reactions at different temperatures ranging from 303 K to 343 K. The rate constant k at different temperatures was calculated from the slope of the linear parts of the different curves. According to the Arrhenius plots ($\ln k$ versus $1/T$), the activation energy value E_a is calculated to be 52.07 kJ mol⁻¹.

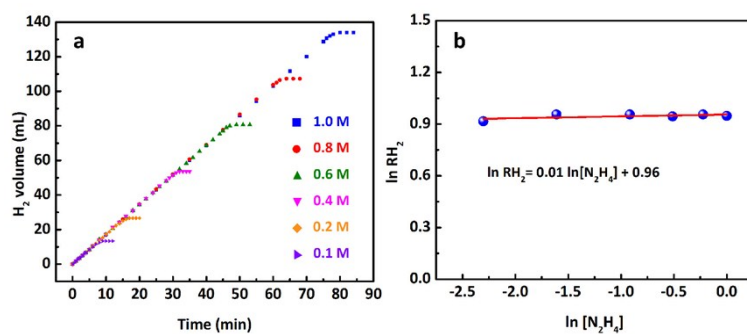


Fig. S6 (a) Plots of volume of evolved hydrogen versus time during the hydrazine decomposition over NF73 at different hydrazine concentrations ($[Ni] = 0.2271 \text{ M}$, $T = 333 \text{ K}$). (b) Plots of $\ln[RH_2]$ versus $\ln[N_2H_4]$ during the hydrazine decomposition over NF73 at different hydrazine concentrations ($[Ni] = 0.2271 \text{ M}$, $T = 333 \text{ K}$).

Fig. S6 shows the plots of evolved hydrogen volume versus time over NF73 at different hydrazine concentrations ranging from 0.1 to 1.0 M under 333 K. Hydrazine concentrations ($[N_2H_4]$) have no obvious effect on the rate of hydrogen generation. Therefore, the reaction rate (RH_2), which was calculated from the linear part of the hydrogen generation plot for each hydrazine concentration, was used for constructing the reaction rate versus hydrazine concentrations plot in a logarithmic scale. A slope of nearly-zero suggests that the kinetic of hydrous hydrazine decomposition accords with zero order model.

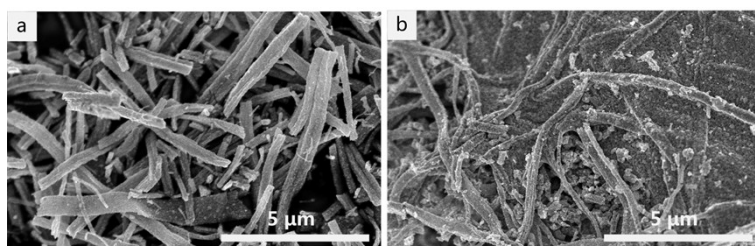


Fig. S7 SEM images of NF73 after (a) one cycle and (b) five cycles.

The durability of NF73 catalyst was investigated by a five-run test. As shown in Fig. S7, Ni nanofibers were cracked, while their fibroid shapes were still maintained. Even after five cycles, NF73 showed a recognizable morphology, indicating the good stability of the catalyst.

Table S1 Comparison of catalytic performances of different catalysts for hydrogen generation from the decomposition of hydrous hydrazine.

Catalyst	T (K)	TOF (h ⁻¹)	Selectivity (%)	Reference
Ni/MIL-101-NH ₂	298	1.3	—	3
Ni/Al ₂ O ₃	303	2.2	93	4
Ni ₉₀ Rh ₁₀	323	3.3	100	5
NiFe	343	4.2	100	6
Ni _{0.95} Ir _{0.05}	333	4.4	100	7
Rh ₄ Ni	298	4.8	100	8
Ni/CeO ₂ -HH-2 (68 wt% Ni)	323	5.1	95	9
Ni _{0.60} Pd _{0.40}	343	5.5	82	10
NiCo/NiO–CoO _x	298	5.9	99	11
Ni _{0.9} Pd _{0.1}	298	6.4	100	12
NF73	333	6.9	100	This work
Cu@Fe ₃ Ni ₅	343	11.9	100	13

There are many nickel-based catalysts with excellent catalytic performances. However, preparation of these nickel-based catalysts requires complex synthesis procedures, multistep treatment and even noble metals. In our work, nickel nanofibers catalyst was prepared by a simple method and possesses good catalytic activity when compared with some nickel-based catalysts.

References

- 1 V. Rosca, M. Duca, M. T. d. Groot and M. T. M. Koper, *Chem. Rev.*, 2009, **109**, 2209.
- 2 S. K. Singh, X. B. Zhang and Q. Xu, *J. Am. Chem. Soc.*, 2009, **131**, 9894.
- 3 P. L. Liu, X. J. Gu, Y. Y. Wu, J. Cheng and H. Q. Su, *Int. J. Hydrogen Energy*, 2017, **42**, 19096.
- 4 L. He, Y. Q. Huang, A. Q. Wang, X. D. Wang, X. W. Chen, J. J. Delgado and T. Zhang, *Angew. Chem., Int. Ed.*, 2012, **51**, 6191.
- 5 A. K. Singh, M. Yadav, K. Aranishi and Q. Xu, *Int. J. Hydrogen Energy*, 2012, **37**, 18915.

- 6 S. K. Singh, A. K. Singh, K. Aranishi and Q. Xu, *J. Am. Chem. Soc.*, 2011, **133**, 19638.
- 7 S. K. Singh and Q. Xu, *Chem. Commun.*, 2010, **46**, 6545.
- 8 S. K. Singh and Q. Xu, *J. Am. Chem. Soc.*, 2009, **131**, 18032.
- 9 W. Kang and A. Varma, *Appl. Catal. B*, 2018, **220**, 409.
- 10 X. B. Chen, H. Q. Wang, S. Gao and Z. B. Wu, *J. Colloid. Intref. Sci.*, 2012, **377**, 131.
- 11 D. D. Wu, M. Wen, X. J. Lin, Q. S. Wu, C. Gu and H. X. Chen, *J. Mater. Chem. A*, 2016, **4**, 6595.
- 12 H. L. Wang, J. M. Yan, Z. L. Wang, S. O and Q. Jiang, *J. Mater. Chem. A*, 2013, **1**, 14957.
- 13 J. Wang, Y. Li and Y. Zhang, *Adv. Funct. Mater.*, 2014, **24**, 7073.